International Journal of Recent Innovations in Academic Research
E-ISSN: 2635-3040; P-ISSN: 2659-1561
Homepage: https://www.ijriar.com/
Volume-7, Issue-10, October-2023: 60-73

Research Article

Comparative Analysis of Eaton's and Bowel's Methods in Pore Pressure Estimation: Unag Field Offshore Niger Delta

[1]*Ideozu, R.U. and [2]Unuagba, P.T.

[1,2]Department of Geology, University of Port Harcourt, Rivers State, Nigeria
*Corresponding Author Email: richmond.ideozu@uniport.edu.ng

Received: October 03, 2023 **Accepted:** October 22, 2023 **Published:** October 30, 2023

Abstract
The knowledge of pore pressure plays an essential role in the drilling, planning, and production operations in the oil and gas industry. The aim of this research is to estimate pore pressure from well log data of the Unag Field situated Offshore in the Niger Delta Nigeria. The overpressured layers were categorised into three overpressure zones (A, B and C) using velocity and effective stress methods, respectively. The identified overpressure zones vary in thickness across the wells. Results reveal that overpressures were generated by disequilibrium compaction and pore pressures. The results further show that undercompaction (loading) mechanism of overpressure, which is characterised by gradual, and increasing slight overpressure with depth, may be the main cause of overpressure especially in zones A and B across the three wells. The research compares the Eaton's and Bower's pore pressure prediction methods. The Bower's method predicted pore pressure values better than the Eaton's method, which is in close agreement with the actual RFT data for three different zones in the studied wells. Hence, the Bower's method is proposed as useful and a better method for predicting pore pressures in other fields in the Niger Delta Basin using well logs.
Keywords: Pore Pressure Prediction, Eaton's Method, Bower's Method, Abnormal Pressure, Overpressure, Niger Delta.

Introduction

Hydrocarbon bearing formations in many sedimentary basins may be associated with various pressure regimes and pore pressure (formation pressure in the wellbore), effective pressure (rock grain pressure) and overburden pressure (a combination of pore pressure and rock grain pressure). These pressures may be encountered in such formations which have high abnormal formation pore pressures or abnormal formation pressures often called overpressures. Pressure regimes may slightly differ from related sedimentary basins with similar depositional history whereas different overpressure regimes may be experienced in the same formation as a result of variations in geological processes such as compaction disequilibrium (undercompaction), hydrocarbon generation, gas cracking, aqua thermal expansion, tectonic compression (lateral stress), uplift-tectonics, illitization, and osmosis (Swarbrick and Osborne, 1998; Gutierrez *et al.,* 2006). These geological processes may act as mechanisms of overpressure and grouped as loading, unloading or tectonic stress (Cao *et al.,* 2006). Several authors widely use the detection of overpressure zones and statistical model of pore pressure from the log (Zhang, 2011; Singha and Chatterjee, 2014; Azadpour *et al.,* 2015; Chatterjee *et al.,* 2015; Hadi *et al.,* 2019; Paglia *et al.,* 2019) among others.

The Loading mechanism-undercompaction occurs when pore fluids are confined or partially expelled from the pore space of the formation as a result of rapid deposition and sedimentation. During this process, the trapped pore fluids will try to retain the pore space, thus, slowing down the rate of compaction in those undercompacted layers/bed/formation (Chopra and Huffman, 2006). The unloading mechanisms may be caused by fluid expansion, erosional or tectonic uplifts, which unloads the sediments resulting in rapid pore pressure increases. Tectonic stress mechanisms occur in tectonic zones where the rate of fluid expulsion cannot keep up with the rapid increase in tectonic stress induced compaction (Cao *et al.,* 2006). In all cases where under-compaction is the primary cause of overpressure, the age of the rocks is usually geologically young and the pressured rocks in these zones are predominantly late Mesozoic and Tertiary where the depositional setting is mainly deltaic, and shale the dominant lithologic unit, such as in Niger Delta Basin

(Zhang, 2011; Alao *et al.,* 2014). Overpressure prediction is based on the premise that compaction-dependent geophysical logging properties such as sonic, resistivity and density are a proxy for pore pressures. Shales are the primary lithology for overpressure prediction because they respond more to overpressure when compared to other rock types such as sands/sandstones. Thus, pore pressure prediction centers on the deformational behavior of shales/clays. According to Doust and Omatsola (1990), the Niger Delta started evolving when inputs from clastic channels increased and prograded over Continental-Oceanic subsidising lithospheric transition zone and spread into the Oceanic Crust of the Gulf of Guinea during the Oligocene (Adesida *et al.,* 1997). The Niger Delta sediment pile has an average thickness of 12km covering an area approximately 300,000km^2 (Tuttle *et al.,* 1999). River dominated sedimentary processes is understood to have formed the Proto-Niger Delta, after the Oligocene, the delta became associated with wave dominated sediments forming well-developed shoreface sands, tidal channels, beach ridges, freshwater and mangrove swamps.

The Niger Delta is one of the largest basins in the world with an upward transition from the Akata Marine Shales (with lenses of very fine grained) through the Agbada sand/shale sequence to the continental Benin Sands which experienced phases of regressions and transgression. According to Kulke (1995), when rifting ceased in the Niger Delta during the Late Cretaceous, gravity tectonics became the primary deformational process and shale mobility brought about internal deformation that resulted to shale diaparism caused by loading of under-compacted Akata Shales by the high density Agbada parallic sand-shale sequence. Depobelts formed when paths of sediment supply were restricted by patterns of structural deformation, which focused sediment accumulation into restricted areas on the delta. Such depobelts changed position over time as local accommodation was filled, and the locus of deposition shifted basinward (Doust and Omatsola, 1990). In all depobelts of the Niger Delta, gravity deformation ended before the formation of the Benin Formation. Gravity deformation which took place in the Niger Delta were characterised by complex structures in the form of steeply dipping, carefully space flank faults, collapsed growth faults, shale diapirs, anticlines and roll over anticlines (Doust and Omatsola, 1990). Normal faults formed by gravity deformation triggered by the movement of deep-seated, overpressured, ductile, marine shale deformed much of the Niger Delta clastic sedimentary wedge (Doust and Omatsola, 1990) and many of these faults were formed during the progradation affecting sediment dispersal.

Fault growth was accompanied by slope instability along the continental margin, which flattened with depth into a detachment plane (s) near the top of the overpressured marine shales at the base of the Agbada Formation. The fault structure balance was distinctive at sections of the Agbada Formation and straightens into separation planes down to the Akata Formation (Evamy *et al.,* 1978; Xiao and Suppe, 1992). Relevant researches on pore pressure prediction in the study area are those of Hospers (1965); Weber and Daukoru (1975); Ekweozor and Daukoru (1984); Brun *et al.,* (1985); Kogbe (1989); Starcher (1995); Reijers *et al.,* (1997); Opara and Onuoha (2009); Nfor and Ndicho (2011); Ugwu and Nwankwo (2014); Ojo *et al.,* (2017) and Previous authors have reported that the Niger Delta is well known to be associated with various pressure regimes and which is typically related to overpressure produced by disequilibrium compaction and unloading (Alao *et al.,* 2014; Eze *et al.,* 2018; Unuagba *et al.,* 2021; Unuagba and Ideozu, 2022). Consequently, it is important to be aware of the magnitude of the formation pressure in this zone before spudding an exploration well. The knowledge of pore pressure will avoid catastrophes like kicks, blowouts, caving–in, and loss of circulation, loss of life and properties, environmental pollution. Hence the motivation of this research is to use well logs data to predict and estimate the overpressures in Unag Field. The aim of this research is to compare the Eaton's and Bowers method while the objectives are to predict the overpressure zone (s), estimate the overpressures in Unag Field, and determine the method that work best. The Unag Field is located within the Shallow Offshore Depobelt of the Niger Delta and see Figure 1.

Materials and Methods

Materials

The data sets used in this research was provided by an International Oil Company in Nigeria through the Department of Petroleum Resources (DPR) a subsidiary Nigerian National Petroleum Corporation (NNPC) which for propriety reasons the name of Company will not be disclosed. The data set provided comprise Wireline log data (Sonic, Density, Resistivity and Gamma Ray logs) and Check shot data.

Methods

The methods used in this research comprises data QA/QC, importation of data, seismic data analysis, pore pressure prediction and pore pressure estimation, and the delineation of overpressure zones. See Figure 1.

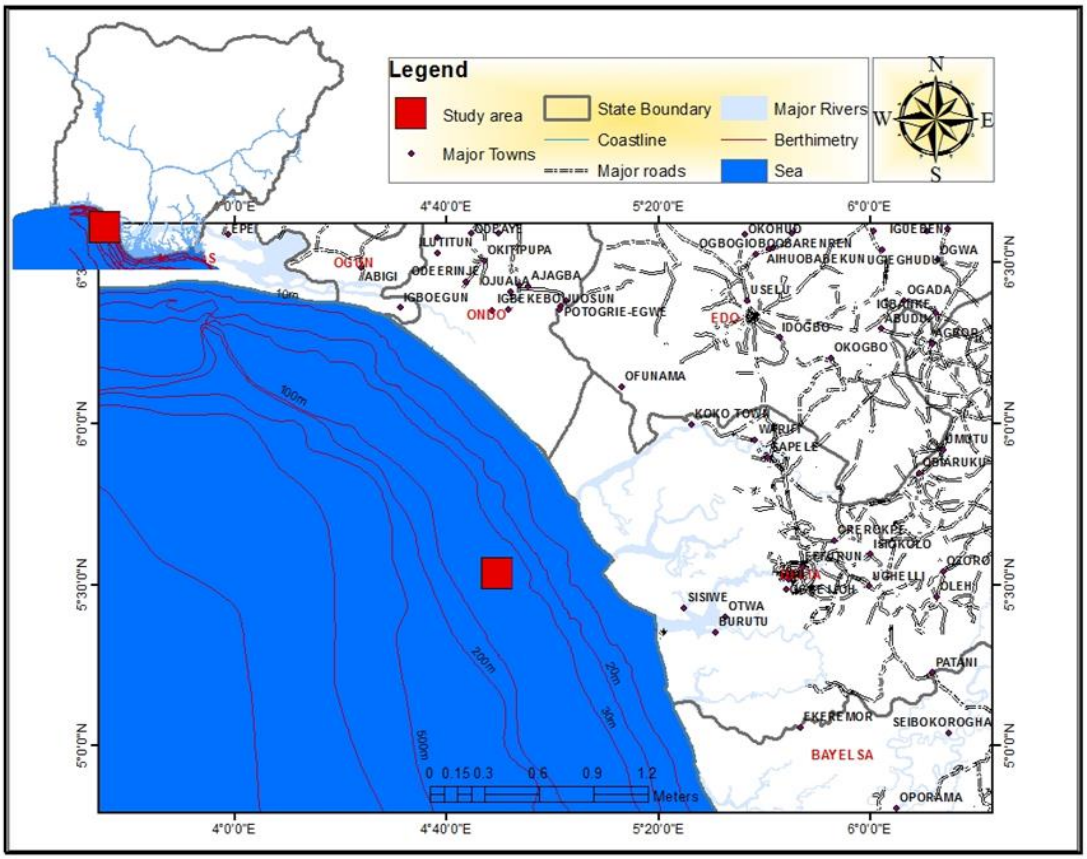

Figure 1. Study area location (After Unuagba, 2019).

Data Quality Checking (QA/QC)

The process of data quality check and control commences with Microsoft notepad to crosscheck the well coordinates, arrange the depth and inclination information, well header, deviation data and surface elevation data before they are imported into RokDoc software. The editing process began by removing the sections of the data which had negative values. The remaining data were sorted and rearranged into columns to maintain its default uniform consistency.

Pore Pressure Prediction Methods from Well Logs

Overpressure may be predicted directly from the velocity of the sonic log by identifying velocity reversals from the normal velocity travel trend. At the same time, effective stress may be derived from density log by identifying the reduction in effective stress from the overburden trend, reduction in density and increase/decrease in effective stress magnitude of sand or shale (Pressure cell method) as depth increases.

Effective Stress/Pressure Cell Method

Effective stress/pressure are pressures exerted on the rock matrix, while pressure cells are volumes of specific sediments that approximately have the same overpressure (Wodu *et al.,* 2014). From these definitions, it is believed that the pressure cells of sands are different from the pressure cells of shales and these two different rock types make up approximately 80% of siliciclastics in the formation under study (Agbada Formation). Thus, because effective pressure is the combination of all the pressure cells in the formation, the pressure cell method was used to isolate the pressures on shales from that of sand in this research. This was achieved by generating a 2D overburden trend which shows the effective stress (sand/shale pressure cells) of the formation. The 2D overburden trend was generated by integrating density best fit line with de-spiked density logs from wells by employing the equation of bulk density as a function of depth;

$$Rho(bml) = Rho_{ma} - \left(Rho_{ma} - Rho_{Top}\right) * \exp(-b * TVDBML) \qquad 1$$

Where; $Rho(bml)$–sediment bulk rock density as a function of depth below the mud line, Rho_{ma}–matrix density (g/cc); 2.565g/cm^3, Rho_{Top}–sediment density at mudline (g/cc), b–compaction coefficient; 0001524, and $TVDBML$ – true vertical depth below the mud line (m)

And overburden pressure equation;

$$\sigma V = \rho b \times D \times g \qquad 2$$

Modified from Terzaghi, (1943) where; σV–overburden stress, ρb–is the average bulk density, D–vertical depth from datum (seafloor for offshore and land surface for onshore) and g– gravitational constant.

The 2D overburden delineated the effective stress of in–situ bulk density of spudded wells. Pressure cells for both sand and shale have been represented by contrasting colours and separated by "exponential density best fit line". The colour contrast for the rock types may changes as the entire rock matrix reacts to compaction. Shale volume logs were generated from the Gamma Ray logs for the three well logs and were juxtaposed with the 2D overburden trend to delineate overpressure.

Velocity Determination Method from Vp (Compressional Velocity Logs)

According to Chopra and Huffman (2006), pore pressure increases with depth in formation evaluation tools such as sonic velocities (Vs or Vp), resistivity and density logs. Overpressures may be predicted from these logs because of the influence such properties as resistivity, sonic, density and porosity have on compaction. During sedimentation and burial, rock grains compact leading to increase in effective stress (increase in bulk and shear modulus of rock grains; as a result of to increased grain contact area and stress respectively), decrease in porosity and increase in density. This process is continuous unless a mechanical process such as stiffness of rock grain or pore pressure (in this case, overpressure) reduces the rate of compaction (Chopra and Huffman, 2006).

In areas of high seal integrity or low permeable rocks such as shale, overpressure build-ups may not escape from the formation, leading to undercompaction. The process of undercompaction does not stop porosity loss and increase in density; instead, it slows down the rate of porosity reduction and density increase. On well logs, undercompaction intervals will slightly deviate or still follow the normal compaction trend (NCT). However, the rocks within these conditions will exhibit "lower velocity" and high porosity when compared to rocks at the same depth of burial under normal compaction conditions (Chopra and Huffman, 2006).

In unloading scenario, the overpressure stops compaction abruptly, unlike the case for undercompaction (Chopra and Huffman, 2006). Furthermore, there is no further loss of porosity and a continuous increase in bulk density. When the overpressure in this zone is so high, it reduces the grain contact stress between rock grains and significantly reduces the acoustic properties (because of sonic velocity travel by grain to grain contact) (Huffman and Bowers, 2002; Chopra and Huffman, 2006). If the grain contact is drastically reduced without any further increase in porosity or decrease in bulk density, this may suggest unloading and may be identified from well logs by sharp velocity deflection below the normal increasing trend combined with non-increasing density (Chopra and Huffman, 2006) (See Figure 4). Unloading mechanism for overpressure may be identified from the velocity-density cross plot (Figure 5). It displays how velocity significantly increases, peaks (in loading scenarios) and gradually reduces while density remains the same (for unloading events).

Pore Pressure Estimation Method

The empirical equations of (Terzaghi, 1943; Eaton, 1975; Bowers, 1995) methods have been used to estimate the overpressures predicted from Effective stress and compressional velocity in Unag Field. The Eaton's method is a widely used method for pressure estimation which utilizes resistivity/sonic velocity data by comparing in-situ physical properties (resistivity or velocity) to normally compacted property at the same depth. The Bowers empirical method accounts for the case where overpressures are caused by the unloading mechanism prevalent in the Agbada Formation. Unloading intervals are zones of (effective) stress in which the effective stress reduces and is maintained at a low level without any significant increase in porosity or reduced density from density logs (Chopra and Huffman, 2006).

Terzaghi Overburden Stress Determination (Terzaghi, 1943)

Conventional methods of overpressure estimation are derived from the theory of compaction, which relates pore pressure to the physical properties of a formation. The fundamental assumption of Terzaghi's original equation analyses compaction caused by overburden stress, see equation 3.

$$\sigma V = \sigma e + P \quad (3)$$

Where overburden stress-(σv), pore pressure-(P) and effective stress-(σe). By rearranging Equation 3, it is possible to calculate the overpressure in shales if the overburden and effective stress are known/estimated using equation 4.

$$\sigma V - \sigma e = P \quad (4)$$

The overburden stress can also be calculated directly from density log data. See equation 2.

Equation (3) and Figure 6 demonstrate that Overburden stress σV increases with depth in a formation, expelling formation fluids in the process as a result of compaction. If pore pressure (P) remained normal when P equals hydrostatic pressure from 500ft to 2000ft also if effective stress σe increases continually (normally), it does so because the weight of the formation is supported mainly by the rock matrix from 500ft – 2250ft. When formation fluids are trapped, pore pressure P increases abnormally as overburden pressure (σV) increases from 2500ft– 3700ft and effective stress reduces.

Eaton's Transit Time Method (Eaton, 1975)

In 1975, Eaton devised an approach for relating acoustic velocity to formation pore pressure in well logs. The following is a derivative of Eaton's method used and applied in this research;

From Terzaghi's equation (3) Eaton deduced;

$$P = \sigma V - \sigma e \quad (5)$$

After that, he established a relationship between the sonic log and measured pressure data in clean shale;

$$P = \Delta to - \Delta tn \quad (6)$$

Where Δto = observed sonic transit time in shale and Δtn = normal transit travel time in shale

Since log parameters are a function of P, σv, and σe respectively,

$$P = \sigma V - \sigma e \left[\frac{\Delta tn}{\Delta to}\right]^{3.0} \quad (7)$$

Eaton developed an empirical relationship which predicted overpressure behaviour with effective stress constant;

$$P = \sigma V - 0.535\left[\frac{\Delta tn}{\Delta to}\right]^{3.0} \quad (8)$$

From equation (8) when σe = 0.535(effective stress constant), overburden pressure (σv) and change in transit time in the formation (transit time ratio [Δtn/Δto]) = 1, the formation will be normally pressured (Pn).

$$Pn = 1 - 0.535(1.0)^{3.0} = 0.465\text{psi/ft} \quad (9)$$

Rearranging equation (5), effective stress is in normal geopressure situation;

$$\sigma e = \sigma V - Pn \quad (10)$$

However, equation (8) shows that in abnormal geopressure situations, the effective stress is approximately;

$$\sigma e = 0.535\left[\frac{\Delta tn}{\Delta to}\right]^{3.0} \quad (11)$$

From equation (11) effective stress (σe) = 0.535 when there is a normal change in transit travel time it signifies normal pressure i.e. when $\Delta tn/\Delta to$ = 1. Thus, if equation (11) is substituted into equation (10) (Which proves; $\sigma e = 0.535$ (effective stress constant in normal pressured events) when $Pn = 0.465 psi/ft$ and $\left[\frac{\Delta tn}{\Delta to}\right]^{3.0} = 1$), effective stress can be directly related to acoustic values of clean shale as follow;

$$\sigma e = \sigma v - Pn\left[\frac{\Delta tn}{\Delta to}\right]^{3.0} \quad (12)$$

Equation (5) shows abnormal pore pressure prediction is a function of the difference of overburden pressure and effective stress but in equation (11) effective stress (σe) functions as a proxy for prediction of formation pore pressure because, effective stress (σe) is directly proportional to the overburden weight (as overburden increases, effective stress increases) but if the effective stress is abnormally low when the weight of overburden is high at a particular depth, it therefore indicates overpressure, thus, in this scenario, Pore pressure can be estimated with equations (5)–if the overburden and effective stresses are known, and equation (12)–because effective stress magnitude is inversely proportional to pore pressure (low effective stress results to overpressure vice versa) but Eaton combined the aforementioned equations to account for the estimation of both normal and overpressure conditions by substituting equation (12) into equation (5) which was applied in this research;

$$P = \sigma V - (\sigma V - Pn)\left[\frac{\Delta tn}{\Delta to}\right]^{3.0} \quad 13$$

(Eaton's empirical formula for estimating overpressure)

Bowers Method (1995)

Bowers, (1994), through his equation, estimated unloading, under-compaction and normal compaction from a single equation which may be used to calibrate existing well data. The Bowers empirical equation was applied to this research for overpressure estimation;

Bowers (1995), calculated overburden pressure and effective stress from pore pressure derived from equation (5), his formula is as follows;

$$Vp = Vml + A\sigma e^{B} \quad 14$$

Where Vp = compressional velocity at any depth, Vml = mudline compressional velocity, σe = effective stress, A and B = calibrated parameters with the offset velocity versus effective stress (σe). Rearranging equation (14) with respect to equation (9) ($\sigma e = \sigma V - P$), the pore pressure is calculated from the velocity (Vp) as;

$$P = \boldsymbol{\sigma}\mathrm{v} - \left(\frac{(Vp - Vml)}{A}\right)^{\frac{1}{B}} \quad 15$$

Bowers modified equation (15) in terms of sonic transit time by replacing $10^6/\Delta$t for Vp and $10^6/\Delta tml$ for Vml;

$$P = \sigma\mathrm{v} - \left(\frac{10^{6\left(\frac{1}{\Delta \mathrm{t}} - \frac{1}{\Delta tml}\right)}}{A}\right)^{\frac{1}{B}} \quad 16$$

Where Δtml is the mudline Vp transit time, normally Δtml =200 μs/ft or 660 μs/m.

When unloading occurs, compressional velocity (Vp) and effective stress do not follow the normal loading curve, and according to Bowers (2002), higher velocity than the velocity in the loading curve will appear at the same effective stress in the event of unloading thus, Bowers (1995), gave the following equation to account for unloading:

$$Vp = Vml + A\left[\sigma \max\left(\frac{\sigma e}{\sigma max}\right)^{\frac{1}{u}}\right]^{B} \quad 17$$

Where σe, Vp, Vml, A and B still represent their parameters above, "U" represents the uplift parameter (unloading); and

$$\sigma \max = \left(\frac{Vmax - Vml}{A}\right)^{\frac{1}{B}} \quad 18$$

Where σmax and Vml represents estimates of effective stress and velocity at the inception of unloading. In the absence of significant lithological changes, Vmax is calibrated to equal the velocity at the onset of the velocity reversal.

Rearranging equation (17) overpressure can be calculated from the unloading event with the following equation;

$$Pulo = \sigma v - \left(\frac{vp - vml}{A}\right)^{\frac{U}{B}} (\sigma\max)^{1-U} \quad 19$$

Pulo = unloading overpressure.

Results and Discussion

Normal Compaction Trend (NCT) of Shale Zone and Tops of Overpressure (TOV)

The first step adopted was to establish the normal compaction trend and the top of overpressure and then compare results of Eaton and Bower's pore prediction methods to determine which of the methods that best conform to the data. The normal compaction trend for each well was derived from the compressional (Vp) sonic velocity logs in Figure 2 to 4. Interpretation of the plots are based on significant deviations from the normal compaction trend which signifies the onset of overpressure in the Wells under study.

Three tops of overpressure (TOV1, TOV2 and TOV3) was identified from wireline logs (Unag 001–003 respectively), and these overpressure tops across the wells were correlated in Figure 5. Overpressure tops for Unag 001 occurred at depths of 7600ft, 9200ft and 10500ft respectively, see Figure 2. In Unag 002 well, overpressure tops occurred at a depth of 81000ft, 8700ft and 10300ft, see Figure 3. Lastly, overpressure tops for Unag 003 occurred at depths of 8000ft, 10000ft and 11800ft respectively, see Figure 4.

Velocity Determination for Overpressure

The result of overpressure prediction from velocity determination is presented in Figures 5 to 10. We now look at individual wells and analyse the response.

Well Unag 001

Three overpressure zones were identified based on reduced velocity signatures from the normal velocity travel trend, see Figure 5. The overpressured zones were designated as; A (7600ft–8800ft), B (9200ft–10100ft) and C (10500ft–11000ft). Under compaction (disequilibrium compaction) is believed to be the cause of overpressure in A and B because the velocity trend slightly deflected away from the normal compaction trend in the depths of overpressure zones aforementioned. At C, there was a sharp deflection from the normal compaction trend and the magnitude of deflection in Figure 2 was larger than the deflections in overpressure zones A and B, thus the cause of overpressure may be related to unloading. The identification of the cause of overpressure across the wells was based on Chopra and Huffman (2006) identification technique.

Well Unag 002

The velocity travel trend normally increased with depth in Unag 002 (Figure 6); however, there was a slight reduction in velocity signatures at 8100ft–8500ft, 8700ft–9700ft and 10300ft–11000ft respectively which represents the only overpressure zones existent in this well and has been designated as A, B and C. The magnitude of decreased velocity from the normal travel trend is relatively low in A and B when compared to C see Figure 6. Invariably overpressures magnitudes in A and B are just slightly above normal pressure in overpressured zones (A and B). Disequilibrium compaction (undercompaction) is identified as the cause of overpressure in Unag 002 based on Chopra and Huffman, (2006) techniques.

Well Unag 003

Three overpressured zones have been identified in Unag 003, they are A (8000ft–9000ft), B (10000ft–10500ft) and C (11800ft–12700ft) see Figure 7. Velocity signatures slightly deviated away from the normal travel trend in overpressure zone A, which indicates mild overpressure. In overpressure zone B, there was a significant deflection of velocity signatures away from the normal travel trend, while in overpressure zone C, the velocity deflection from the normal travel trend was steep and at this depth also, shale density remained constant in the overburden trend. The steep velocity deflection indicates high overpressures, and when combined with the density scenario, it is believed that the cause of overpressure points to unloading (Chopra and Huffman, 2006).

Comparison of Eaton's and Bower's Overpressure Estimation

In order to select the best pore pressure prediction method, a comparison between the Eaton and Bower methods with RFT (See Figure's 8 to 10) for Zones A, B and C in the studied wells was undertaken. The results from Bower's pore prediction method shows better agreement compared when to the Eaton's

method. Eaton's and Bowers empirical models were used to estimating overpressures in Unag 001–003wells. The estimated overpressure in each zone (overpressure zones) was plotted against depth using Microsoft excel scatter chart to show the range of pressure magnitude in each zones across the three wells using normal pressure as a benchmark for the onset of overpressure. Loading events consists of a continuous increase of the overburden stress identified on velocity–density cross plot by a slow but continuous increase in effective stress, density and velocity (See Figure 10).

In the unloading events, compaction is brought to a halt (Chopra and Huffman, 2006) and it is identified by sharp velocity reversal and abrupt standstill of density i.e. density stops increasing because the load is either carried entirely by the pore fluids or uplifts must have occurred (See Figure 8 and 10). The Bowers (1995) method for pore pressure prediction using an effective stress approach, is based on the relationship between velocity and effective stress. In the zones where overpressure was generated by undercompaction mechanisms, overpressure can be predicted using Bowers loading/virgin curve, whereas, in the zone where the fluid expansion mechanism is present, overpressure can be predicted using Bowers unloading curve (Bowers, 1995).

The overpressure analysis of Unag 001, 002 and 003 wells, using three methods that is the effective stress/pressure cell method, velocity method and the empirical method predicted the overpressures in the overpressured zones. The magnitudes of these overpressures were estimated using Eaton's and Bowers empirical models. Pressure cells from the overburden trend are a specific to a group of sediments that have the same effective stress (rock pressure) while the effective stress is the pressure of the entire sediments in a formation. The results of the effective stress/pressure cell method showed a reduction in density of shales and reduction in effective stress of the entire formation as depth increases which are indicators of overpressure.

The velocity method predicted overpressure from velocity reversals from the normal velocity travel trend or normal compaction trend (NCT) and from this method, three overpressure zones A, B and C were identified across the wells. Overpressure zone C has the highest velocity reversal (indicating high overpressures) most notably from 10500ft–12700ft across the wells in the field. Under-compaction and unloading, is believed to be the primary overpressure mechanism in the Niger Delta, defined from velocity reversal and changes in density using Chopra and Huffman method of identifying overpressure mechanism from well logs.

Under-compaction mechanism yielded low to mild overpressure, and they are the primary mechanism of overpressure. Unloading mechanism like fluid expansion and tectonics produced high overpressures, and are believed to be secondary mechanisms generating overpressure. The most important cause of overpressure across the three wells was under-compaction, but in overpressure zone C of Unag, well 001 and 003 unloading mechanism was the cause of overpressure because it was characterised by sharp velocity reversal with zero density increase in shale as depth increases. The Eaton's and Bowers empirical methods evaluated the overpressure magnitude across the wells in pounds per square inch (psi). The estimates of overpressure range (Eaton's method) in UNAG 001 overpressure zones A, B and C are 4121.6psi–5747.3psi, 5405psi–6229.7psi and 71622psi–8785.8psi respectively. The estimate of overpressure range (from Bower's empirical method) in UNAG 002 overpressure zones A, B and C are 3942.3psi–4807.7psi, 4423.1psi–5528.8psi and 5673.1psi–6923.1psi respectively and the measured overpressure range (Eaton's method) in UNAG 003 overpressure zones are 3576.5psi–4779.4psi, 5073.5psi–6323.5psi and 6176.5psi–86618psi respectively.

Correlation of overpressure zones and structural interpretation (Unuagba, 2019) determined the cause of overpressures (as under-compaction or unloading) in the wells. Undercompaction mechanism is suggested as the primary cause of overpressure in overpressure zones A and B of the field. The results show that field is associated with mild overpressures caused by under-compaction across the wells. In addition, the Bower's method predicted pore pressure values better than the Eaton's method, which is in close agreement with the actual RFT data for three different zones in the studied wells.

Conclusion

The research compares the Eaton's and Bower's pore pressure prediction methods. The Bower's method predicted pore pressure values which are in close agreement with the actual RFT data for three different zones in the wells studied compared to the Eaton's method. It is proposed that Bower's method be used in predicting pore pressure from other oil fields in the Niger Delta Basin.

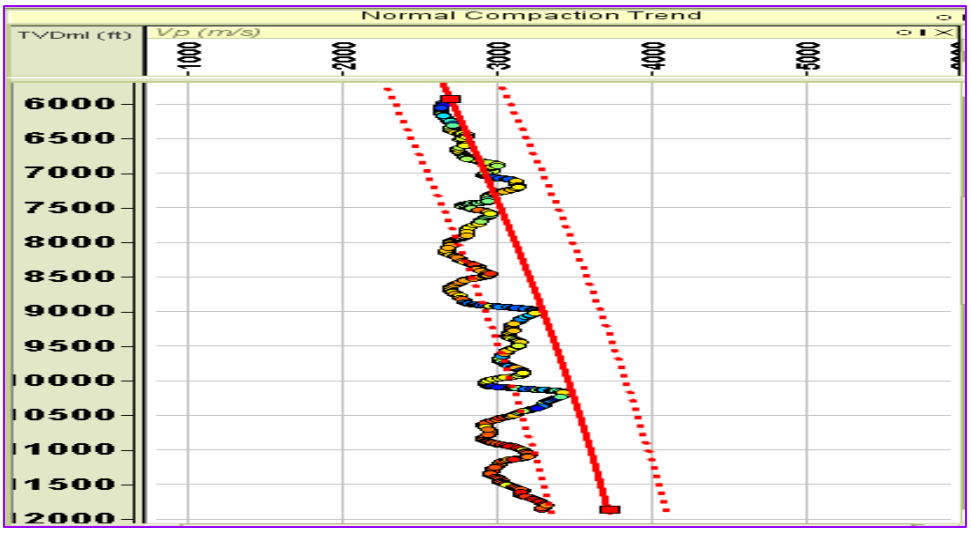

Figure 2. Normal compaction trend (NCT) from compressional sonic velocity (Vp) log showing top of overpressure in Unag 001 (RokDoc software, 2010 version).

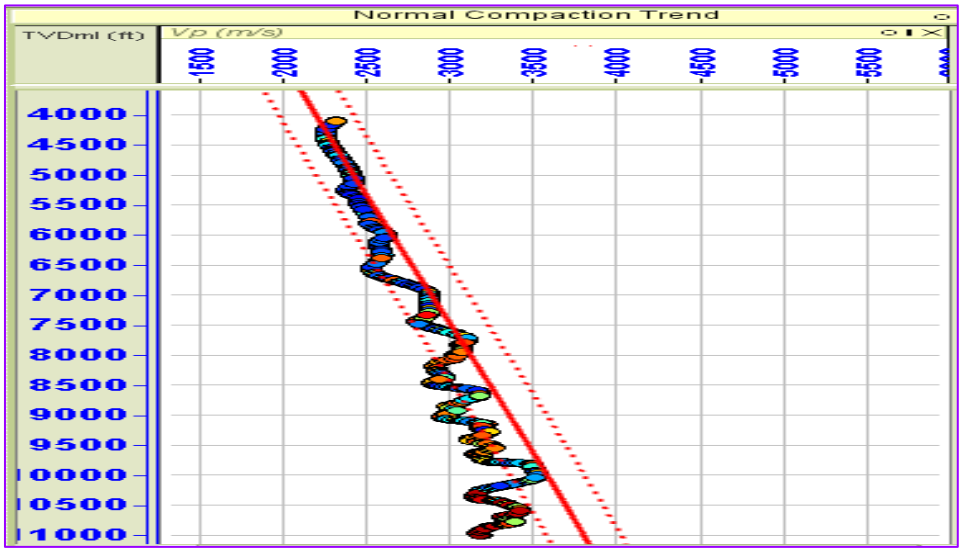

Figure 3. Normal compaction trend (NCT) from compressional sonic velocity (Vp) log showing top of overpressure in Unag 002 (RokDoc software, 2010 version).

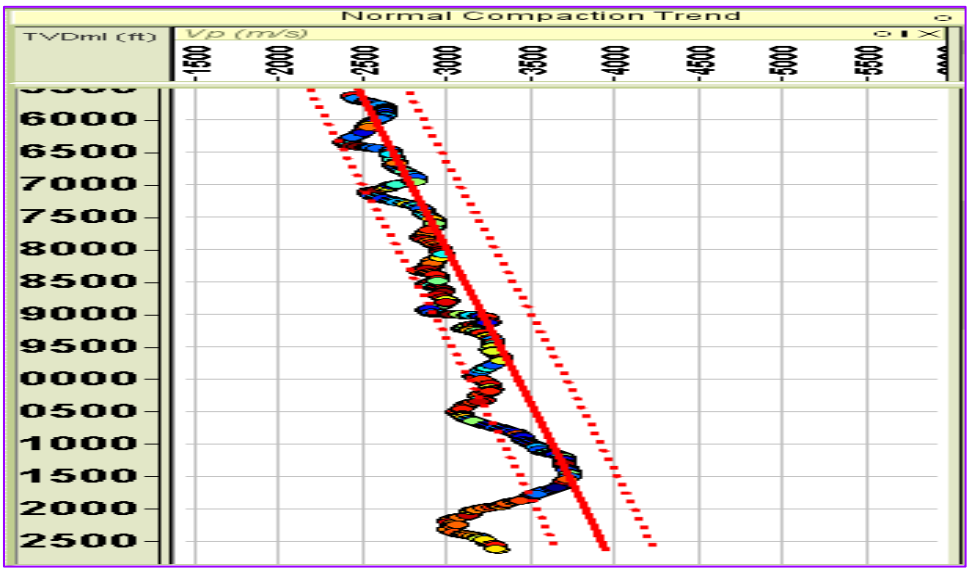

Figure 4. Normal compaction trend (NCT) from compressional sonic velocity (Vp) log of Unag 003 (RokDoc software, 2010 version).

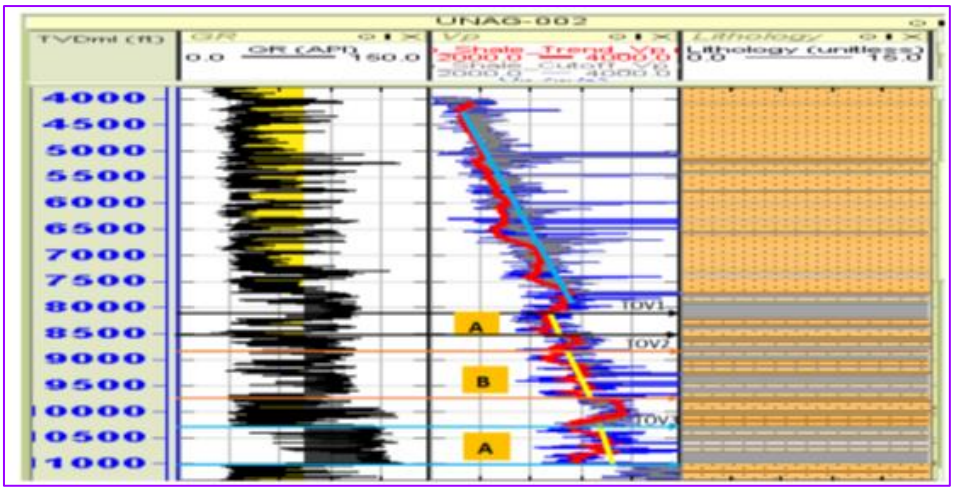

Figure 5. Velocity and gamma ray logs showing top of overpressure (TOV1-TOV3), overpressure zones (A, B and C) and rock physical properties of normal compaction (blue trend line), disequilibrium compaction/under-compaction (yellow trend line) for Unag 002 (RokDoc software, 2010 version).

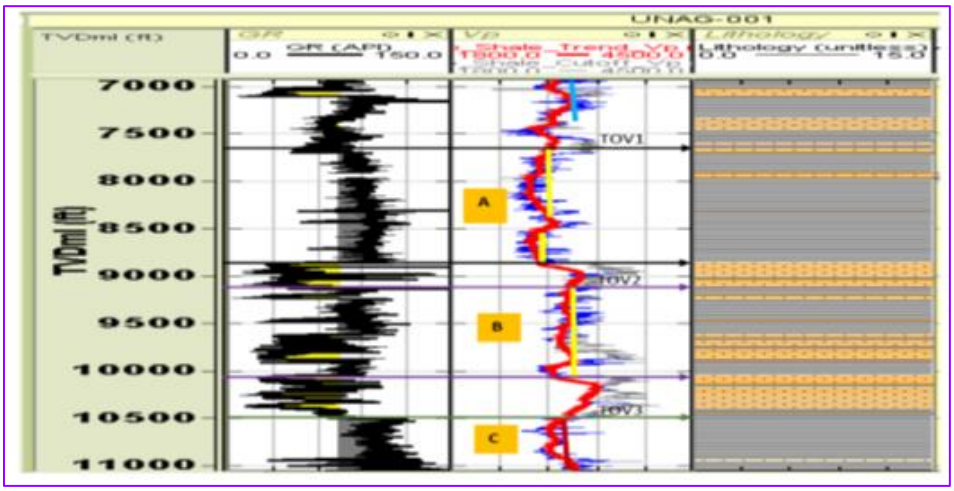

Figure 6. Velocity and gamma ray logs showing top of overpressure (TOV1-TOV3), overpressure zones (A, B and C) and rock physical properties of normal compaction (blue trend line), disequilibrium compaction/under-compaction (yellow trend line) and unloading (red trend line) for Unag 001 (RokDoc software, 2010 version).

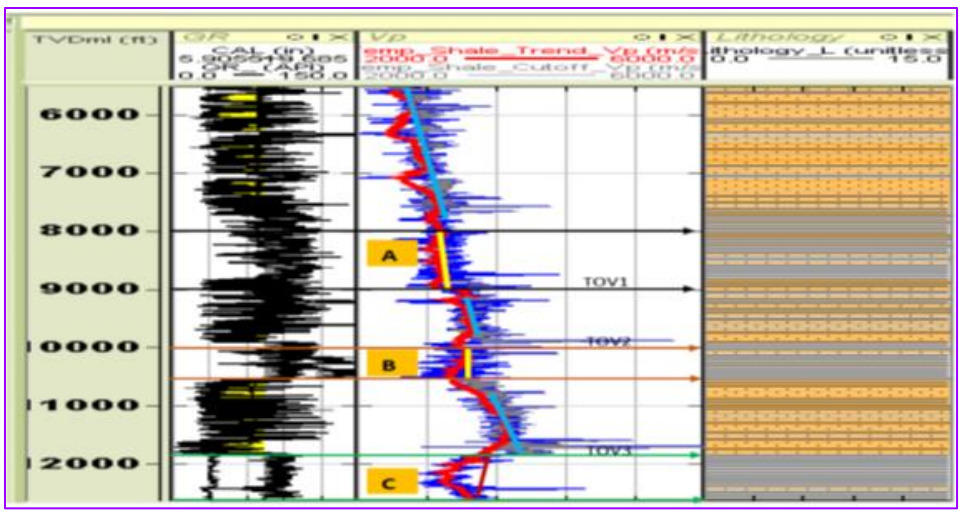

Figure 7. Velocity and gamma ray logs showing top of overpressure (TOV1-TOV3), overpressure zones (A, B and C) and rock physical properties of normal compaction (blue trend line), disequilibrium compaction/under-compaction (yellow trend line) and unloading (red trend line) for Unag 003 (RokDoc software, 2010 version).

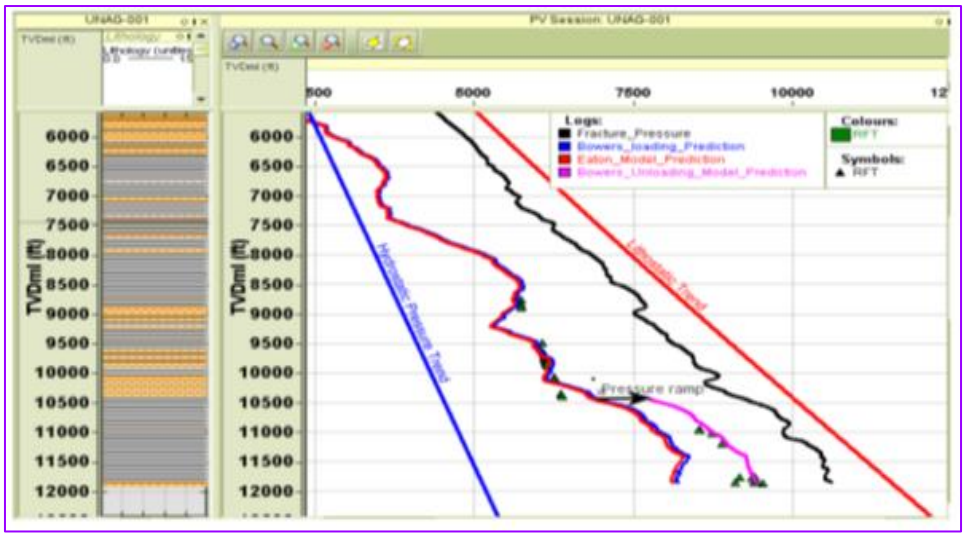

Figure 8. Eaton's and Bowers empirical models showing estimates of overpressures in Unag 001 well (RokDoc software, 2010 version).

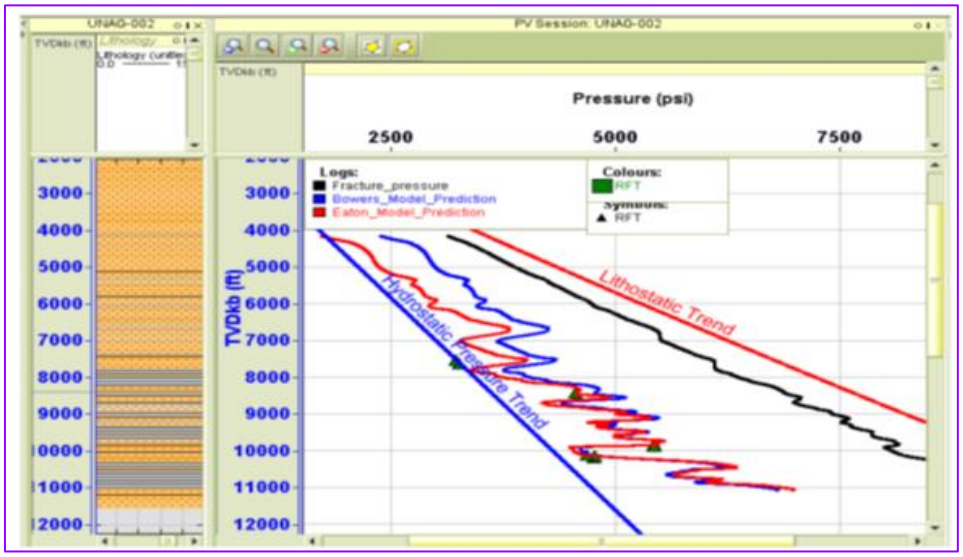

Figure 9. Eaton's and Bowers empirical models showing estimates of overpressures in Unag 002 well (RokDoc software, 2010 version).

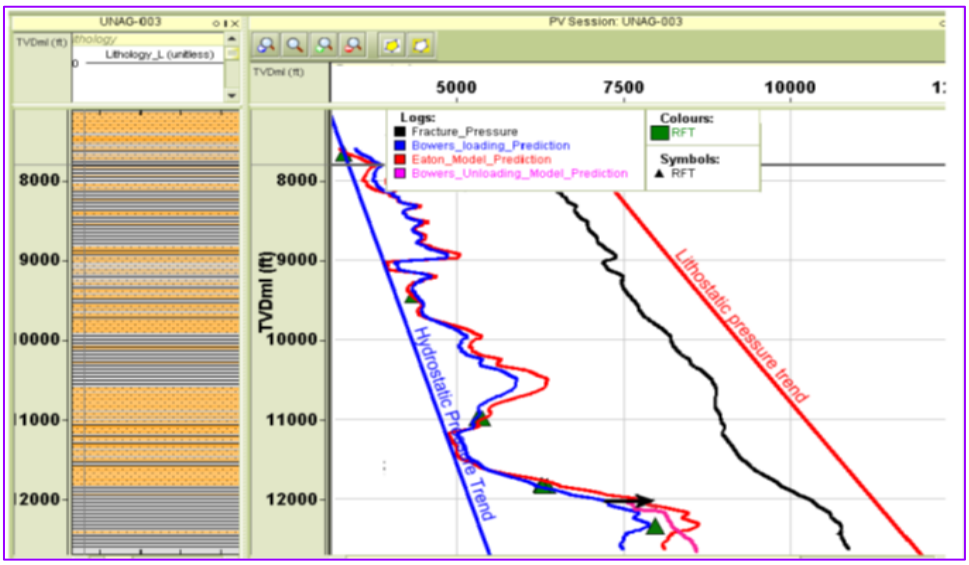

Figure 10. Eaton's and Bowers empirical models showing estimates of overpressures in Unag 003 well (RokDoc software, 2010 version).

Declarations

Acknowledgements: This work is an extract from the M.Sc. dissertation of Mr. P.T. Unuagba supervised by R.U. Ideozu (PhD). The dissertation is titled 'Overpressure Prediction and Estimation in Unag Field Niger Delta Using Well Log and Seismic Data'. The authors are grateful to the Department of Petroleum Resources (DPR) now Nigerian Upstream Regulatory Commission (NUPRC) for assisting in the provision of the data used in this research.

Author Contributions: The author (s) confirms sole responsibility for the following: study conception and design, data collection, analysis and interpretation of results, and manuscript preparation.

Conflict of Interest: The authors declare no conflict of interest.

Consent to Publish: The authors agree to publish the paper in International Journal of Recent Innovations in Academic Research.

Data Availability Statement: Not applicable.

Funding: This research received no external funding.

Institutional Review Board Statement: Not applicable.

Informed Consent Statement: Not applicable.

Research Content: The research content of manuscript is original and has not been published elsewhere.

References

1. Adesida, A.A., Reijers, T.J.A. and Nwajide, C.S. 1997. Sequence stratigraphic framework of the Niger delta. In: Proceedings of the AAPG International Conference and Exhibition.
2. Alao, O., Ofuyah, W. and Abegunrin, A. 2014. Detecting and predicting over pressure zones in the Niger delta Nigeria: a case study of Afam field. Journal of Environment and Earth Science, 4(6): 13-20.
3. Azadpour, M., Manaman, N.S., Kadkhodaie-Ilkhchi, A. and Sedghipour, M.R. 2015. Pore pressure prediction and modeling using well-logging data in one of the gas fields in south of Iran. Journal of Petroleum Science and Engineering, 128: 15-23.
4. Bowers, G.L. 1994. Pore pressure estimation from velocity data: accounting for overpressure mechanisms besides undercompaction. In: 1994 IADC/SPE Drilling Conference, 515–530pp.
5. Bowers, G.L. 1995. Pore pressure estimation from velocity data: accounting for overpressure mechanisms besides undercompaction. SPE Drilling and Completion, 10(02): 89-95.
6. Bowers, G.L. 2002. Detecting high overpressure. Leading Edge, 21(2): 174–177.
7. Brun, S., Grivelet, P. and Paul, A. 1985. Prediction of overpressure in Nigeria using vertical seismic profile techniques. In: SPWLA 26th Annual Logging Symposium: Society of Petrophysicists and Well-Log Analysts.
8. Cao, S., Xie, Y., Liu, C., Yan, G., YI, P., Cai, J. and Xu, L. 2006. Multistage approach on pore pressure prediction-a case study in the South China Sea. In: International Oil and Gas Conference and Exhibition in China: Society of Petroleum Engineers.
9. Chatterjee, R., Paul, S., Singha, D.K. and Mukhopadhyay, M. 2015. Overpressure zones in relation to in situ stress for the Krishna-Godavari basin, the eastern continental margin of India: implications for hydrocarbon prospectivity. In: Petroleum Geosciences: Indian Contexts, Springer, 127–142pp.
10. Chopra, S. and Huffman, A.R. 2006. Velocity determination for pore-pressure prediction. The Leading Edge, 25: 1502–1515.
11. Doust, H. and Omatsola, E. 1990. Divergent/passive margin basins. AAPG Memoir, 48: 239–248.
12. Eaton, B.A. 1975. The equation for geopressure prediction from well logs. In: Fall Meeting of the Society of Petroleum Engineers of AIME: Society of Petroleum Engineers.
13. Ekweozor, C.M. and Daukoru, E.M. 1984. Petroleum source-bed evaluation of tertiary Niger delta: reply. AAPG Bulletin, 68: 390–394.
14. Evamy, B.D., Haremboure, J., Kamerling, P., Knaap, W.A., Molloy, F.A. and Rowlands, P.H. 1978. Hydrocarbon habitat of tertiary Niger delta. AAPG Bulletin, 62: 1–39.
15. Eze, S., Ideozu, R.U., Abel, I.T., Jacob, O.A. and Wasiu, O.O. 2018. Unloading mechanism: an indication of overpressure in Niger delta ('X'-field) using cross plots of rock properties. International Journal of Research in Social Sciences, 8: 719–736.

16. Gutierrez, M.A., Braunsdor, N.R. and Couzens, B.A. 2006. Calibration and ranking of pore-pressure prediction models. The Leading Edge, 25: 1516–1523.

17. Hadi, F., Eckert, A. and Almahdawi, F. 2019. Real-time pore pressure prediction in depleted reservoirs using regression analysis and artificial neural networks. In: SPE Middle East Oil and Gas Show and Conference: Society of Petroleum Engineers.

18. Hospers, J. 1965. Gravity field and structure of the Niger delta, Nigeria, West Africa. Geological Society of America Bulletin, 76: 407–422.

19. Huffman, A.R. and Bowers, G.L. 2002. Pressure regimes in sedimentary basins and their prediction: AAPG Memoir 76 (Volume 76). AAPG.

20. Kogbe, C.A. 1989. The Cretaceous and Paleogene sediments of southern Nigeria. Geology of Nigeria, 2: 325-334.

21. Kulke, H. 1995. Regional petroleum Geology of the World. Part II: Africa, America, Australia and Antarctica. Lubrecht and Cramer Ltd., Berlin, 143-172.

22. Nfor, B. and Ndicho, O.M.I. 2011. Porosity as an overpressure zone indicator in an X-field of the Niger delta basin, Nigeria. Archives of Applied Science Research, 3: 29–36.

23. Ojo, A.O., Adepelumi, A.A. and Ojo, OA.A. 2017. Abnormal pressure detection using integrated approach in "Oluku" field, East Niger-Delta, Nigeria. Journal of Geography, Environment and Earth Science International, 9(3): 1-11.

24. Opara, A.I. and Onuoha, K.M. 2009. Pre-drill pore pressure prediction from 3-D seismic data in parts of the onshore Niger delta basin. In: Nigeria Annual International Conference and Exhibition: Society of Petroleum Engineers.

25. Paglia, J., Eidsvik, J., Grøver, A. and Elisabet Lothe, A. 2019. Statistical modelling for real-time pore pressure prediction from predrill analysis and well logs. Geophysics, 84: ID1–ID12.

26. Reijers, T.J.A., Petters, S.W. and Nwajide, C.S. 1997. The Niger delta basin. In: Sedimentary Basins of the World. Elsevier, 151–172 pp.

27. Singha, D.K. and Chatterjee, R. 2014. Detection of overpressure zones and a statistical model for pore pressure estimation from well logs in the Krishna-Godavari basin, India. Geochemistry, Geophysics, Geosystems, 15: 1009–1020.

28. Starcher, P. 1995. Present understanding of the Niger delta hydrocarbon habitat. In: Oti, M.N. and Postma, G. (Eds.), Geology of Deltas: Rotterdam, AA Balkema, 257–267pp.

29. Swarbrick, R.E. and Osborne, M.J. 1998. Memoir 70, Chapter 2: Mechanisms that Generate Abnormal Pressures: An Overview.

30. Terzaghi, K. 1943. Theoretical soil mechanics. John Wiley and Sons. New York, 11–15.

31. Tuttle, M.L., Charpentier, R.R. and Brownfield, M.E. 1999. The Niger delta petroleum system: Niger delta province. Nigeria, Cameroon, and Equatorial Guinea, Africa: USGS Open-File Report, 99–50.

32. Ugwu, S.A. and Nwankwo, CN.N. 2014. Integrated approach to geopressure detection in the X-field, onshore Niger delta. Journal of Petroleum Exploration and Production Technology, 4: 215–231.

33. Unuagba, P.T. 2019. Overpressure prediction and estimation in Unag field Niger delta using well log and seismic data. Unpublished M.Sc. Dissertation: Department of Geology, University of Port Harcourt, Nigeria.

34. Unuagba, P.T. and Ideozu, R.U. 2022. Using Bowels' and Eaton's methods to predict and estimate pore pressure in Unag field offshore Niger delta. Proceedings of the 57th NMGS Annual International Conference and Exhibition, Garden City, 3: 495–515.

35. Unuagba, T.P., Ideozu, R.U., Eze, S., Osung, E.W. and Abolarin, O.M. 2021. Prediction of overpressure using effective stress and velocity trend methods in Unag field offshore Niger delta. International Journal of Research and Innovation in Applied Sciences: 6(1): 134-145.

36. Weber, K.J. and Daukoru, E.M. 1975. Petroleum geological aspects of the Niger delta. Paper, I presented at the Ninth World Petroleum Congress, Tokyo.

37. Wodu, E.K., Sarker, R. and Itua, O.J. 2014. Modelling seismic velocities and pressure cells for pre-drill pore pressure prediction and application in development wells in Nigerian deepwater turbidites. In: SPE Nigeria Annual International Conference and Exhibition: Society of Petroleum Engineers.

38. Xiao, H. and Suppe, J. 1992. Origin of Rollover (1). AAPG Bulletin, 76: 509–529.

39. Zhang, J. 2011. Pore pressure prediction from well logs: methods, modifications, and new approaches. Earth-Science Reviews, 108: 50–63.

Citation: Ideozu, R.U. and Unuagba, P.T. 2023. Comparative Analysis of Eaton's and Bowel's Methods in Pore Pressure Estimation: Unag Field Offshore Niger Delta. International Journal of Recent Innovations in Academic Research, 7(10): 60-73.